

Received: 2017.12.18  
Accepted: 2018.04.04  
Published: 2018.04.21

# Intravoxel Incoherent Motion Diffusion-Weighted Imaging of Primary Rectal Carcinoma: Correlation with Histopathology

Authors' Contribution:  
Study Design A  
Data Collection B  
Statistical Analysis C  
Data Interpretation D  
Manuscript Preparation E  
Literature Search F  
Funds Collection G

ABCDEF 1 **Baolan Lu**  
BCDF 1 **Xinyue Yang**  
ABDF 2 **Xiaojuan Xiao**  
BF 1 **Yan Chen**  
ACD 3 **Xu Yan**  
ADG 1 **Shenping Yu**

1 Department of Radiology, The First Affiliated Hospital of Sun Yat-Sen University, Guangzhou, Guangdong, P.R. China  
2 Department of Radiology, Peking University Shenzhen Hospital, Shenzhen, Guangdong, P.R. China  
3 MR Collaboration NE Asia, Siemens Healthcare, Shanghai, P.R. China

**Corresponding Author:** Shen-ping Yu, e-mail: yushp@mail.sysu.edu.cn

**Source of support:** This study was supported by the Project of Guangdong Province Science and Technology Plan (2014A020212126)

**Background:** Comprehensive and precise assessment of rectal carcinoma is crucial before surgery to plan an individual treatment strategy. New functional techniques, such as intravoxel incoherent motion (IVIM), have emerged and could lead to more detailed information. The aim of this study was to evaluate the difference between the rectal tumor parenchyma and normal wall by IVIM and to explore the correlations of IVIM parameters and histopathology.





**Material/Methods:** We prospectively enrolled 128 patients with pathologically proven rectal non-mucinous carcinoma with differentiation degree and 16 patients with mucinous carcinoma. All patients underwent routine MR examination and IVIM sequence. The IVIM maps were automatically generated and 3 ROIs were drawn on the maximal rectal tumor parenchyma and normal rectal wall. The Wilcoxon signed rank test, *t* test, Mann-Whitney U test, and Spearman's rank correlation test were performed.

**Results:** All IVIM parameters demonstrated the difference between rectal tumor parenchyma and normal wall ( $P_D < 0.001$ ;  $P_{D^*} = 0.014$ ;  $P_f < 0.001$ ). Poorly differentiated carcinoma had a significantly lower *f* value ( $P_f = 0.049$ ) than well/moderately-differentiated carcinoma. In addition, mucinous carcinoma had a higher *D* ( $P_D = 0.001$ ) and a lower *D\** value ( $P_{D^*} = 0.001$ ) than non-mucinous carcinoma. Correlation analysis between IVIM parameters and histopathology showed that *D* ( $|r| = 0.538$ ,  $P_D = 0.000$ ) and *D\** ( $|r| = 0.267$ ,  $P_{D^*} = 0.001$ ) had statistically significant correlations with histological type and *f* ( $|r| = 0.175$ ,  $P_f = 0.048$ ) was significantly correlated with differentiation degree.

**Conclusions:** The IVIM parameters of rectal tumor parenchyma and normal wall were significantly different. *D* appears to be a valid and promising parameter to indicate histological features of rectal carcinoma.

**MeSH Keywords:** **Colorectal Neoplasms • Diffusion of Innovation • Magnetic Resonance Imaging**

**Full-text PDF:** <https://www.medscimonit.com/abstract/index/idArt/908574>

 2406  3  4  42



## Background

Colorectal cancer is one of the most common malignant tumors in the world. Over the past few decades, its incidence has been increasing gradually in certain countries where it had historically been low [1]. The prognosis of primary rectal carcinoma is associated with TNM staging and the differentiation degree, which has been repeatedly proven to be an independent prognostic factor [2,3]. Furthermore, a recent meta-analysis [4] indicated that mucinous rectal carcinoma responded poorly to preoperative chemoradiotherapy. Therefore, a comprehensive preoperative assessment of rectal carcinoma is necessary for patient counseling and clinical decision-making.

International guidelines recommended MRI as crucial method for primary staging and restaging of rectal carcinoma after chemotherapy and radiation therapy (CRT) [5–8]. Previous studies [9,10] showed that high-resolution MRI accurately detected anatomical changes in rectal and perirectal tissues. Moreover, functional MRI indirectly indicate biological behavior and help oncologists predict therapeutic effects and assess the prognosis [5,11].

Intravoxel incoherent motion diffusion-weighted imaging (IVIM DWI) is a functional technology that can simultaneously provide information regarding blood microcirculation in the capillary network (perfusion) and diffusion, without requiring an intravenous contrast agent [12]. Studies in the literature [13] have confirmed that the IVIM parameters (pure molecular diffusion coefficient [D], pseudo-diffusion coefficient [D\*], and perfusion fraction [f]) are important surrogate biomarkers to provide information about tissue physiology, with applications in evaluating liver fibrosis [14], transplanted kidney function [15], breast lesions [16,17] and pancreatic diseases [18–20]. Notably, IVIM parameters, especially the perfusion-related parameters (D\*, f) reflecting tissue microcirculation, have emerging clinical applications for resolving diagnostic dilemmas, differentiation of tumor stages and histological types [21–23], and response to neoadjuvant chemoradiotherapy of malignant tumors [24–26].

However, only a few studies used IVIM DWI to assess rectal carcinoma [26–28]. Given the importance of differentiation degree and histological type for preoperative assessment, the purpose of our study was to investigate the clinical application of IVIM DWI for primary rectal carcinoma and, further, to quantitatively analyze the efficacy of IVIM DWI parameters for identifying tumor histopathology to provide a foundation for future studies on rectal carcinoma.

## Material and Methods

### Patients

In accordance with the ethics guidelines for human research, this prospective study was approved by our Institutional Ethics Review Board and informed consent was obtained from all patients. Inclusion criteria were: (1) underwent colonoscopy and suspected as primary rectal carcinoma; (2) underwent conventional high-resolution rectal MRI and IVIM DWI sequences; and (3) had surgery about 2–7 days after MR examination, except those who required neoadjuvant therapy. Exclusion criteria were: (1) lack of pathology results; (2) neoadjuvant therapy was administered before MR examination; (3) pathologically proven as not rectal carcinoma; (4) recurrent carcinoma; (5) the tumor did not have a sufficiently large parenchyma area for selecting ROIs; and (6) the image quality was unsatisfactory without anisodamine injection.

### MR examination

The rectal MR examination was performed using a 3T MRI scanner (Magnetom Verio; Siemens Healthcare, Erlangen, Germany) equipped with an 8-channel body-matrix coil. All patients were routinely intramuscularly injected with 20 mg of anisodamine to minimize intestinal peristaltic movement. This agent has a short half-life and is therefore was injected 5–10 min before the examination. Prior to the initial MRI scan, 30–120 ml of ultrasound gel was injected into the rectum to make the boundary of tumor displayed more clearly. Gadolinium (gadopentetate dimeglumine; Kangcheng; Guangzhou, China) was intravenously injected using a power injector (Medrad, Pittsburgh, PA, USA) at 0.2 mmol/kg body weight at a rate of 3.0 ml/s.

Conventional rectal MRI included axial (TR/TE, 3000/87 ms; FOV, 260×260 mm; 5-mm slice thickness; 25 slices; dist. factor 20%; phase oversampling 70%; voxel size 0.8×0.7×5.0 mm; averages=2; concatenation=2; TA 2 min 56 s), sagittal (TR/TE, 3000/87 ms; FOV, 180×180 mm; 3-mm slice thickness; 19 slices; dist. factor 0%; phase oversampling 70%; voxel size 0.7×0.6×3.0 mm; averages=2; concatenation=2; TA 2 min 30 s) and coronal (TR/TE, 4000/77ms; FOV, 220×220 mm; 3 mm slice thickness; 25 slices; dist. factor 0%; phase oversampling 100%; voxel size 0.7×0.6×3.0 mm; averages=2; concatenation=1; TA 2 min 52s) T2-TSE. It also included T1-TSE (TR/TE, 644/12 ms; FOV, 180×180 mm; 3-mm section thickness; 20 slices; dist. factor 0%; phase oversampling 90%; voxel size 0.6×0.6×3.0 mm; averages=2; concatenation=2; TA 3 min 17 s) and T2-TSE (TR/TE, 3000/84ms; FOV 180×180 mm; 3-mm section thickness; 24 slices; dist. factor 0%; phase oversampling 70%; voxel size 0.7×0.6×3.0 mm; averages=2; concatenation=2; TA 3 min 18 s) perpendicular to the long axis of the rectum covering the whole tumor.

A prototype DWI sequence (TR/TE, 3800/74.7 ms; FOV 300×245 mm; 6-mm section thickness; slab group 1; 21 slices; dist. factor 20%; voxel size 2.7×2.7×6.0 mm; averages=2; concatenation=1; TA 6 min 1 s) was performed prior to gadolinium injection to acquire the IVIM data. A total of 14 b values (0, 5, 10, 20, 30, 40, 60, 80, 100, 150, 200, 400, 600, and 1000 s/mm<sup>2</sup>) were applied using a single-shot spin-echo echo-planar-imaging sequence. The lookup table of gradient directions was modified accordingly to enable multiple b-value measurements in a single series.

### IVIM DWI analysis

The data set was analyzed on the basis of the bi-exponential IVIM DWI model introduced by Le Bihan [29] using the following equation:  $S_b/S_0 = (1-f)\exp(-bD) + f\exp[-b(D^*)]$ , where  $S_b$  is the signal intensity at the particular b-value used,  $S_0$  is the signal intensity at the b-value of 0,  $f$  is the fraction of diffusion linked to microcirculation,  $D$  is the true diffusion coefficient representing molecular diffusion of pure water, and  $D^*$  represents perfusion-related incoherent microcirculation, known as the pseudo-diffusion coefficient.

IVIM DWI data were post-processed using software developed in-house (MatLab Version 2.1; MathWorks, Natick, MA, USA), and the parameter maps of IVIM DWI ( $D$ ,  $f$ , and  $D^*$  parameter maps) were automatically generated in a voxel-by-voxel manner using all 14 b values. A segmented fitting method was used for a more robust calculation, similar to the implementation in a previous study [30].  $D$  and  $f$  were first estimated by assuming the perfusion fraction of signal can be neglected at a b-value >200 s/mm<sup>2</sup>; then,  $D^*$  was calculated by applying the previously calculated  $D$  and  $f$  to the IVIM model.

All ROIs were manually delineated and contoured. The ROI excluded macroscopic necrosis, visible vessels, and gut contents, and was confirmed by comparing the ROI position in the DWI data ( $b=0$  s/mm<sup>2</sup>) to axial T2-weighted imaging. Three ROIs were separately drawn on the maximal rectal tumor parenchyma and normal rectal wall (at a distance from the tumor of over approximately half the circumference of the rectum, without any signs of infiltration). For each ROI, the mean values of  $D$ ,  $f$ , and  $D^*$  were calculated from the corresponding parameter maps, and the resulting values of each parameter from 3 ROIs were then averaged for comparison.

### Histological evaluation

Histological sections from biopsied (non-mucinous:  $n=54$ ) or resected (non-mucinous:  $n=74$ ; mucinous:  $n=16$ ) specimens were evaluated by a pathologist with more than 10 years of experience. The sections were stained with HE (hematoxylin and eosin) stain.

According to the College of American Pathologists [31], rectal carcinomas are stratified into 4 grades: grade 1=well-differentiated (95% of tumor composed of glands), grade 2=moderately-differentiated (50–95% of tumor composed of glands), grade 3=poorly-differentiated (5–49% of tumor composed of glands), and grade 4=undifferentiated (5% of tumor composed of glands). If the rectal carcinoma had mixed degrees of differentiations, the tumor was defined as the highest grade. We combined well- and moderately-differentiated cases into a single group for analysis. Mucinous carcinoma is characterized by abundant extracellular mucin that constitutes more than 50% of the tumor volume.

### Statistical analysis

Descriptive statistics were used to describe clinical demographics using the mean and range.

All measurements of IVIM parameters are expressed as the mean±standard deviation (mean±SD). The Wilcoxon signed rank test was performed to compare the rectal tumor parenchyma and the normal rectal wall. The  $t$  test or Mann-Whitney U test was used to analyze the different differentiations and histological subtypes of rectal carcinoma. Spearman's rank correlation test was performed to analyse the correlations between IVIM parameters and histopathology. All analyses were performed using IBM SPSS Statistics for Windows, Version 20.0 (IBM Cop, Armonk, NY, USA). A 2-tailed  $P$  value of less than 0.05 was considered statistically significant.

## Results

### Patients

In total, we evaluated 128 patients (77 male and 51 female; mean age: 58.5 y; age range: 32–83 y) with rectal non-mucinous carcinoma (poorly-differentiated:  $n=17$ ; moderately-differentiated:  $n=110$ ; well-differentiated:  $n=1$ ) and 16 patients (8 male and 8 female; mean age: 50.1 y; age range: 22–67 y; poorly-differentiated:  $n=7$ ; moderately differentiated:  $n=9$ ) with rectal mucinous carcinoma.

### IVIM parameters

The mean of the largest section of each tumor was (68.23±66.29) mm<sup>2</sup> (range: 10.67–583.33 mm<sup>2</sup>), and the mean normal wall size was (17.01±7.04) mm<sup>2</sup> (range: 5.33–48.67 mm<sup>2</sup>). The measurement results of all IVIM parameters for rectal non-mucinous carcinoma are shown in Table 1. All the IVIM parameters could significantly differentiate rectal tumor parenchyma from the normal rectal wall ( $P_D < 0.001$ ;  $P_{D^*} = 0.014$ ;  $P_f < 0.001$ ). Furthermore, poorly-differentiated non-mucinous carcinoma had a significantly lower  $f$  value than well/moderately-differentiated

**Table 1.** IVIM parameters of non-mucinous rectal tumour parenchyma and normal rectal wall.

IVIM parameters	Rectal tumour parenchyma (mean ±SD) n=128	Normal rectal wall (mean ±SD) n=128	Z	P
D (10 <sup>-3</sup> .mm <sup>2</sup> /s)	0.89±0.09	1.55±0.28	-9.342	<0.001
D*(10 <sup>-3</sup> .mm <sup>2</sup> /s)	14.77±3.67	14.02±7.51	-2.463	0.014
f	0.13±0.03	0.18±0.09	-5.116	<0.001

P<0.05 indicates a statistically significant difference.

**Table 2.** IVIM parameters of moderately/well and poorly differentiated rectal carcinoma.

IVIM parameters	Well/moderately differentiated (mean ±SD) n=111	Poorly differentiated (mean ±SD) n=17	t/Z	P
D (10 <sup>-3</sup> .mm <sup>2</sup> /s)	0.90±0.08	0.87±0.14	0.816	0.425*
D*(10 <sup>-3</sup> .mm <sup>2</sup> /s)	14.91±3.77	13.86±2.82	-0.944	0.345**
f	0.14±0.03	0.12±0.04	-1.969	0.049**

\* Performed by T-test; \*\* performed by Man-Whitney U test. P<0.05 indicates a statistically significant difference.

**Table 3.** IVIM parameters of rectal mucinous and non-mucinous carcinoma.

IVIM parameters	Non-mucinous carcinoma (mean ±SD) n=128	Mucinous carcinoma (mean ±SD) n=16	Z	P
D (10 <sup>-3</sup> .mm <sup>2</sup> /s)	0.89±0.09	1.37±0.23	6.433	<0.001
D*(10 <sup>-3</sup> .mm <sup>2</sup> /s)	14.77±3.67	11.66±4.90	-3.191	0.001
f	0.13±0.03	0.14±0.08	-0.839	0.401

P<0.05 indicates a statistically significant difference.

carcinoma (P=0.049) (Table 2). In addition, mucinous carcinoma had a higher D value (P<0.001) and a lower D\* value (P=0.001) than non-mucinous carcinoma (Table 3).

Examples of the IVIM parameter maps are shown for 1 patient with rectal non-mucinous carcinoma (Figure 1) and for 1 patient with rectal mucinous carcinoma (Figure 2) as examples.

**Correlation analysis**

There was a significant positive correlation between f and differentiation degree (r<sub>f</sub>=0.175, P<sub>f</sub>=0.048). However, D and D\* value negatively correlated with differentiation degree (r<sub>D</sub>=0.073, P<sub>D</sub>=0.412; r<sub>D\*</sub>=0.084, P<sub>D\*</sub>=0.347) (Figure 3).

On the contrary, correlation analysis between IVIM parameters and histopathology showed that D (r<sub>D</sub> =0.538, P<sub>D</sub>=0.000) and D\* (r<sub>D\*</sub>=-0.267, P<sub>D\*</sub>=0.001) had statistically significant correlations with histological type, and f had a negative correlation with histological type (r<sub>f</sub>=-0.0705, P<sub>f</sub>=0.403) (Figure 4).

**Discussion**

A precise preoperative assessment is required for the appropriate surgical management or neoadjuvant therapy of rectal carcinoma. High-resolution MRI currently is part of the clinical routine for preoperative staging [6,32-34], and functional MRI has been receiving increased attention to determine the therapy response and pathological features in rectal carcinoma [5,26,35,36]. In our study, we analyzed differences between the rectal tumor parenchyma and normal rectal wall by IVIM and explored the correlations between IVIM parameters and histopathology to accumulate basic data for clinical applications and expand the use of IVIM for rectal carcinoma.

Our results showed that all IVIM parameters could significantly differentiate the tumor parenchyma from the normal rectal wall, suggesting they are able to reflect changes in the microstructure or microenvironment of tumor tissue. The rectal carcinoma had a significantly lower true diffusion coefficient D than the normal rectal wall, which was in agreement with the



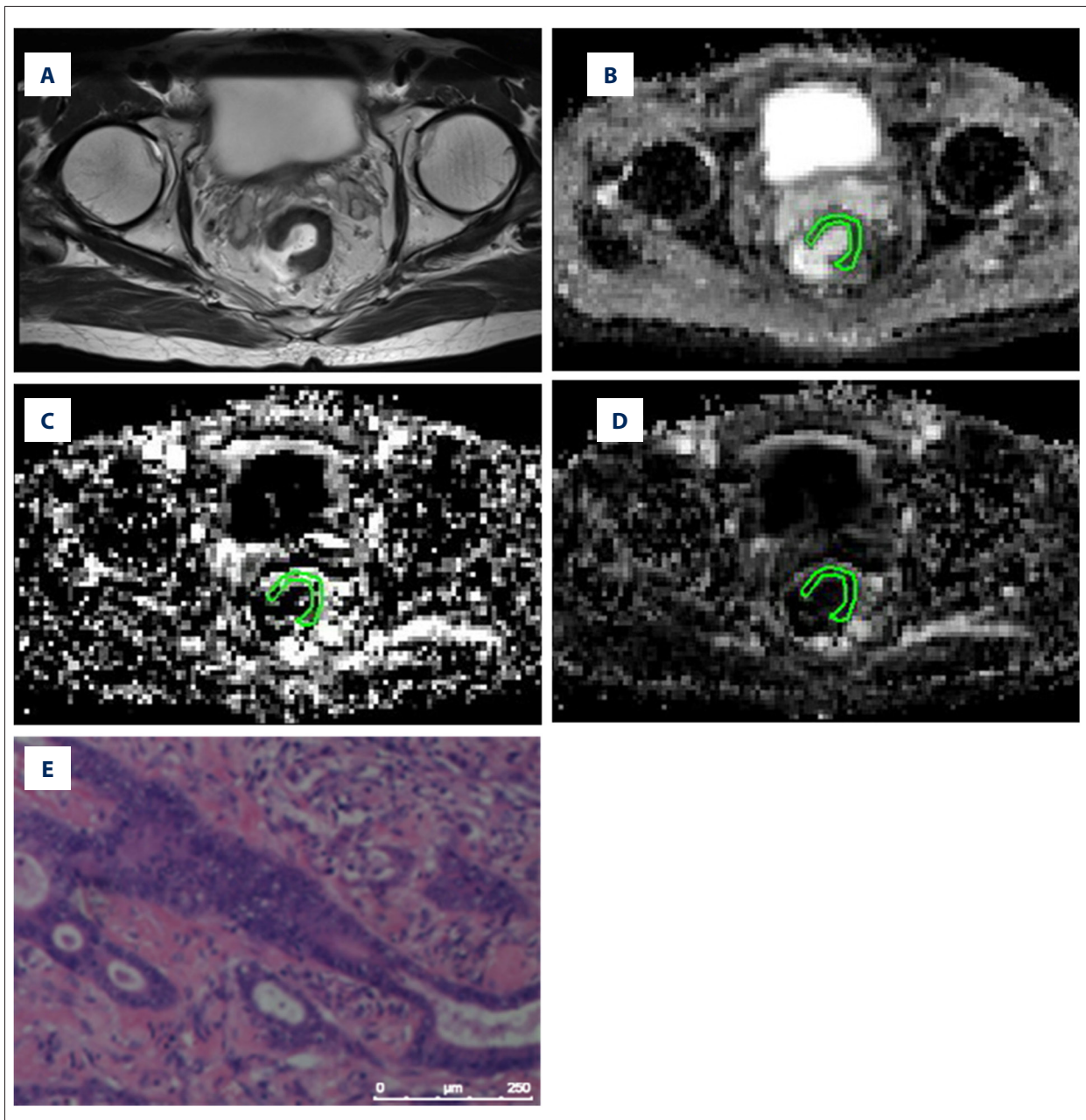


**Figure 1.** A 78-year-old man with rectal non-mucinous carcinoma. (A) Axial T2-weighted image showed a hypointense mass in the rectum. (B–D) The IVIM parameter maps with ROI for quantification and the measured values of D, D\*, and f of the tumor parenchyma were  $0.85 \times 10^{-3} \text{ mm}^2/\text{s}$ ,  $14.24 \times 10^{-3} \text{ mm}^2/\text{s}$ , and 0.15, respectively. (E) HE staining revealed moderately-differentiated rectal non-mucinous carcinoma. Scale bar=250  $\mu\text{m}$ .

results of a previous study [26]. The restricted diffusion may not only be an effect of the increasing cellularity, but also the result of the cellular microstructure or the desmoplastic reaction of the tumor. Moreover, Bauerle et al. [26] concluded that D was more highly associated with the cellular microstructure than with the tumor cellularity. As expected, the perfusion-related D\* value of the tumor parenchyma was significantly higher than those in the normal rectum, which was probably

caused by tumor angiogenesis. However, the tumor parenchyma had a lower f value and this in accordance with the literature [26]. D\* and f seem to be relevant to microcirculation. However, D\* actually reflects the blood flow and may be affected by the flow velocity and vascular geometry, while f represents the effective blood volume [12]. Although the tumor tissue has an abundant blood supply, the structure and function of the tumor vasculature is not perfect. In other words,

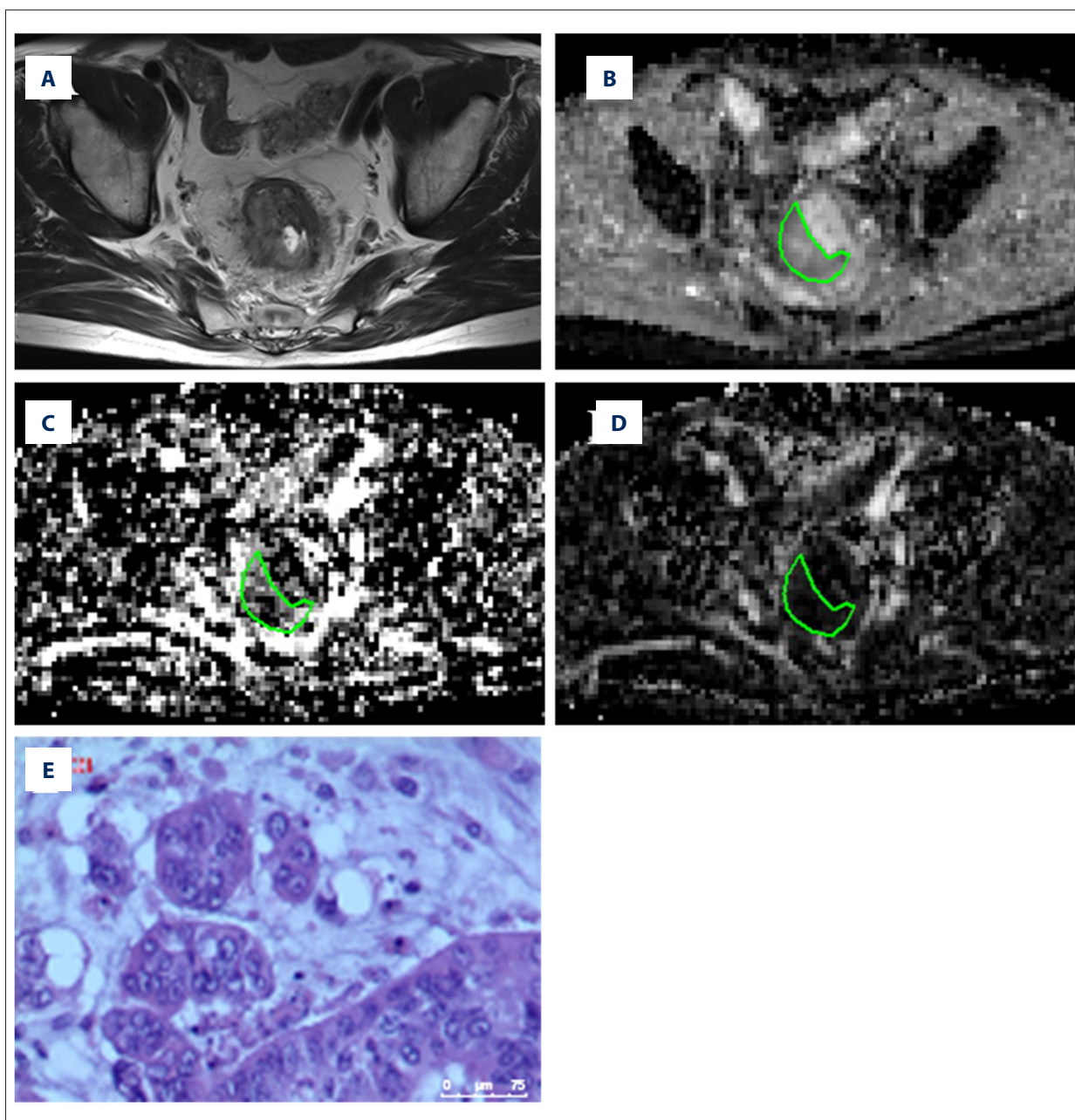


**Figure 2.** A 66-year-old man with rectal mucinous carcinoma. **(A)** Axial T2-weighted image showed a heterogeneous hyperintense mass in the rectum. **(B–D)** The IVIM parameter maps with ROI for quantification and the measured values of  $D$ ,  $D^*$ , and  $f$  of the tumor parenchyma were  $1.44 \times 10^{-3} \text{ mm}^2/\text{s}$ ,  $8.31 \times 10^{-3} \text{ mm}^2/\text{s}$ , and 0.09, respectively. **(E)** HE staining was carried out to assess the histopathology. Scale bar =  $75 \mu\text{m}$ . The mucinous carcinoma is characterized by lakes of mucin containing scant malignant cells.

the chaotic organization, abnormal leakiness, and structural instability of tumor vasculature make few contributions to effective perfusion of microcirculation, leading to a lower value of the measurement of perfusion fraction.

Unexpectedly,  $D$  and  $D^*$  could not clarify the diversity among different differentiated carcinomas. This result was contrary

to the results of a previous study [37] showing that poorly differentiated rectal carcinoma had a lower ADC value. Another study [38] showed that water molecules can move less freely in poorly differentiated tumors due to the increasing cellularity with hydrophobic membrane integrity, extracellular tortuosity, and disorganization, whereas no significant differences were found in  $D$ . Our study only demonstrated a significantly lower  $f$

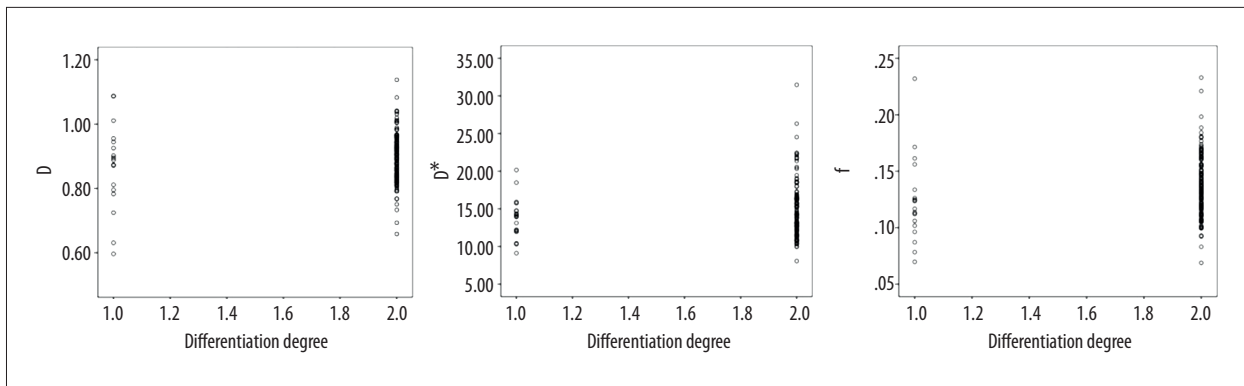


**Figure 3.** Relationship between IVIM parameters and differentiated degree. An increase in the f value was associated with an increase differentiated degree.

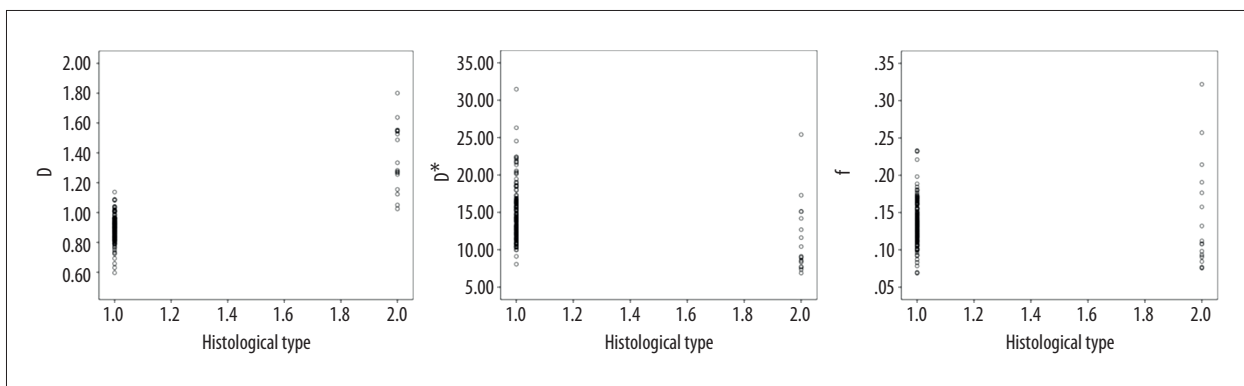


**Figure 4.** Relationship between IVIM parameters and histological type. D and D\* had statistically significant correlations with histological type.

value for poorly-differentiated rectal carcinoma, and the significant positive correlation between f and differentiation degree also indicates this. A possible explanation for this phenomenon is that glandular architecture may be inherently different for each differentiation; tumors of poorly-differentiated degree tended to have fewer glands and glandular architecture may contribute to the measurement of perfusion fraction [39,40].

Recently, a meta-analysis [4] showed that mucinous rectal carcinoma has a poor prognosis and responds poorly to preoperative chemoradiotherapy compared with non-mucinous rectal carcinoma; it is a histological subtype of rectal carcinoma and should be differentiated for adequate treatment [41]. MRI diagnosis of mucinous rectal carcinoma is diagnostically superior to preoperative biopsy [42] by characterizing the hyper-intensity in T2-weighted imaging. In our series of experiments, mucinous rectal carcinoma showed a substantially higher D than in non-mucinous carcinoma, which may be due to the abundant mucin component that decreased the cellularity and facilitated the water molecular deviation. Moreover, we found mucinous rectal carcinoma had a lower D\* than in non-mucinous rectal carcinoma, which may be because the abundant mucin component leads to less microvasculature in the

extracellular matrix. The f values of mucinous and non-mucinous rectal carcinoma were not significantly different. D\* and f are known to lack a simple linear mathematic relationship.

Our study has several limitations. First, all patients had an electronic colonoscopy and biopsy examination before MR examination at different intervals, which may have resulted in bias. Second, single-slice ROI analysis is prone to bias and may not adequately represent tumor heterogeneity. Third, injecting the ultrasound gel into the rectum may enlarge the measurement error in the normal rectal wall. To minimize these limitations, ROIs were drawn on 3 sections at the max levels of the tumor and the normal wall, and the mean value of these 3 ROIs were recorded.

## Conclusions

In conclusion, our study applies IVIM DWI to rectal carcinoma and investigates the IVIM parameters, which can describe the changing microstructure of the tumor tissue. D might be a valid and promising parameter to indicate the histological features of rectal carcinoma. Moreover, D\* can reflect the different



microstructural features in mucinous and non-mucinous rectal carcinoma. The utility of IVIM for distinguishing differentiated rectal carcinoma requires further evaluation.

## References:

- Torre LA, Bray F, Siegel RL et al: Global cancer statistics, 2012. *Cancer J Clin*, 2015; 65: 87–108
- Hermanek P, Guggenmoos-Holzmann I, Gall FP: Prognostic factors in rectal carcinoma. A contribution to the further development of tumor classification. *Dis Colon Rectum*, 1989; 32: 593–99
- Robey-Cafferty SS, El-Naggar AK, Grignon DJ et al: Histologic parameters and DNA ploidy as predictors of survival in stage B adenocarcinoma of colon and rectum. *Mod Pathol*, 1990; 3: 261–66
- McCawley N, Clancy C, O'Neill BD et al: Mucinous rectal adenocarcinoma is associated with a poor response to neoadjuvant chemoradiotherapy: A systematic review and meta-analysis. *Dis Colon Rectum*, 2016; 59: 1200–8
- Prezzi D, Goh V: Rectal cancer magnetic resonance imaging: Imaging beyond morphology. *Clin Oncol (R Coll Radiol)*, 2016; 28: 83–92
- Beets-Tan RG, Lambregts DM, Maas M et al: Magnetic resonance imaging for the clinical management of rectal cancer patients: recommendations from the 2012 European Society of Gastrointestinal and Abdominal Radiology (ESGAR) consensus meeting. *Eur Radiol*, 2013; 23: 2522–31
- Nougaret S, Reinhold C, Mikhael HW et al: The use of MR imaging in treatment planning for patients with rectal carcinoma: Have you checked the "DISTANCE"? *Radiology*, 2013; 268: 330–44
- Nielsen LB, Wille-Jorgensen P: National and international guidelines for rectal cancer. *Colorectal Dis*, 2014; 16: 854–65
- Kaur H, Choi H, You YN et al: MR imaging for preoperative evaluation of primary rectal cancer: Practical considerations. *Radiographics*, 2012; 32: 389–409
- Zhang G, Cai Y, Xu G: Diagnostic accuracy of MRI for assessment of T category and circumferential resection margin involvement in patients with rectal cancer: A meta-analysis. *Dis Colon Rectum*, 2016; 59: 789–99
- Le Bihan D: Apparent diffusion coefficient and beyond: What diffusion MR imaging can tell us about tissue structure. *Radiology*, 2013; 268: 318–22
- Le Bihan D, Breton E, Lallemand D et al: Separation of diffusion and perfusion in intravoxel incoherent motion MR imaging. *Radiology*, 1988; 168: 497–505
- Le Bihan D: Intravoxel incoherent motion perfusion MR imaging: A wake-up call. *Radiology*, 2008; 249: 748–52
- Luciani A, Vignaud A, Cavet M et al: Liver cirrhosis: Intravoxel incoherent motion MR imaging – pilot study. *Radiology*, 2008; 249: 891–99
- Thoeny HC, Zumstein D, Simon-Zoula S et al: Functional evaluation of transplanted kidneys with diffusion-weighted and BOLD MR imaging: Initial experience. *Radiology*, 2006; 241: 812–21
- Sigmund EE, Cho GY, Kim S et al: Intravoxel incoherent motion imaging of tumor microenvironment in locally advanced breast cancer. *Magn Reson Med*, 2011; 65: 1437–47
- Bokacheva L, Kaplan JB, Giri DD et al: Intravoxel incoherent motion diffusion-weighted MRI at 3.0 T differentiates malignant breast lesions from benign lesions and breast parenchyma. *J Magn Reson Imaging*, 2014; 40: 813–23
- Graf M, Simon D, Lemke A et al: Toward a non-invasive screening tool for differentiation of pancreatic lesions based on intra-voxel incoherent motion derived parameters. *Z Med Phys*, 2013; 23: 46–55
- Klauss M, Lemke A, Grunberg K et al: Intravoxel incoherent motion MRI for the differentiation between mass forming chronic pancreatitis and pancreatic carcinoma. *Invest Radiol*, 2011; 46: 57–63
- Kang KM, Lee JM, Yoon JH et al: Intravoxel incoherent motion diffusion-weighted MR imaging for characterization of focal pancreatic lesions. *Radiology*, 2014; 270: 444–53
- Lee EY, Yu X, Chu MM et al: Perfusion and diffusion characteristics of cervical cancer based on intravoxel incoherent motion MR imaging—a pilot study. *Eur Radiol*, 2014; 24: 1506–13
- Lai V, Li X, Lee VHF et al: Nasopharyngeal carcinoma: comparison of diffusion and perfusion characteristics between different tumour stages using intravoxel incoherent motion MR imaging. *Eur Radiol*, 2014; 24: 176–83
- Sumi M, Nakamura T: Head and neck tumours: Combined MRI assessment based on IVIM and TIC analyses for the differentiation of tumors of different histological types. *Eur Radiol*, 2014; 24: 223–31
- Lai V, Li X, Lee VHF et al: Intravoxel incoherent motion MR imaging: comparison of diffusion and perfusion characteristics between nasopharyngeal carcinoma and post-chemoradiation fibrosis. *Eur Radiol*, 2013; 23: 2793–801
- Wang YC, Hu DY, Hu XM et al: Assessing the early response of advanced cervical cancer to neoadjuvant chemotherapy using intravoxel incoherent motion diffusion-weighted magnetic resonance imaging: A pilot study. *Chin Med J (Engl)*, 2016; 129: 665–71
- Bauerle T, Seyler L, Munter M et al: Diffusion-weighted imaging in rectal carcinoma patients without and after chemoradiotherapy: A comparative study with histology. *Eur J Radiol*, 2013; 82: 444–52
- Zhu HB, Zhang XY, Zhou XH et al: Assessment of pathological complete response to preoperative chemoradiotherapy by means of multiple mathematical models of diffusion-weighted MRI in locally advanced rectal cancer: A prospective single-center study. *J Magn Reson Imaging*, 2017; 46: 175–83
- Zhang G, Wang S, Wen D et al: Comparison of non-Gaussian and Gaussian diffusion models of diffusion weighted imaging of rectal cancer at 3.0 T MRI. *Sci Rep*, 2016; 6: 38782
- Le Bihan D, Turner R, MacFall JR: Effects of intravoxel incoherent motions (IVIM) in steady-state free precession (SSFP) imaging: Application to molecular diffusion imaging. *Magn Reson Med*, 1989; 10: 324–37
- Suo S, Lin N, Wang H et al: Intravoxel incoherent motion diffusion-weighted MR imaging of breast cancer at 3.0 tesla: Comparison of different curve-fitting methods. *J Magn Reson Imaging*, 2015; 42: 362–70
- Compton CC, Henson DE, Hutter RV et al: Updated protocol for the examination of specimens removed from patients with colorectal carcinoma. A basis for checklists. *Arch Pathol Lab Med*, 1997; 121: 1247–54
- Moreno CC, Sullivan PS, Kalb BT et al: Magnetic resonance imaging of rectal cancer: Ataging and restaging evaluation. *Abdom Imaging*, 2015; 40: 2613–29
- Tudyka V, Blomqvist L, Beets-Tan RG et al: EURECCA consensus conference highlights about colon & rectal cancer multidisciplinary management: The radiology experts review. *Eur J Surg Oncol*, 2014; 40: 469–75
- Nielsen LB, Wille-Jorgensen P: National and international guidelines for rectal cancer. *Colorectal Dis*, 2014; 16: 854–65
- Mannelli L, Nougaret S, Vargas HA et al: Advances in diffusion-weighted imaging. *Radiol Clin North Am*, 2015; 53: 569–81
- Pham TT, Liney GP, Wong K et al: Functional MRI for quantitative treatment response prediction in locally advanced rectal cancer. *Br J Radiol*, 2017; 90: 1072–78
- Curvo-Semedo L, Lambregts DM, Maas M et al: Diffusion-weighted MRI in rectal cancer: apparent diffusion coefficient as a potential noninvasive marker of tumor aggressiveness. *J Magn Reson Imaging*, 2012; 35: 1365–71
- Liu Y, Ye Z, Sun H et al: Grading of uterine cervical cancer by using the ADC difference value and its correlation with microvascular density and vascular endothelial growth factor. *Eur Radiol*, 2013; 23: 757–65
- Koh DM, Collins DJ, Orton MR: Intravoxel incoherent motion in body diffusion-weighted MRI: Reality and challenges. *Am J Roentgenol*, 2011; 196: 1351–61
- Iima M, Le Bihan D: Clinical intravoxel incoherent motion and diffusion MR imaging: Past, present, and future. *Radiology*, 2016; 278: 13–32
- Dijkhoff RA, Maas M, Martens MH et al: Correlation between quantitative and semiquantitative parameters in DCE-MRI with a blood pool agent in rectal cancer: Can semiquantitative parameters be used as a surrogate for quantitative parameters? *Abdom Radiol (NY)*, 2017; 42: 1342–49
- Yu SK, Chand M, Tait DM et al: Magnetic resonance imaging defined mucinous rectal carcinoma is an independent imaging biomarker for poor prognosis and poor response to preoperative chemoradiotherapy. *Eur J Cancer*, 2014; 50: 920–27

## Conflict of interest

None.